





Cite this: *Mater. Adv.*, 2026,
7, 3315

Aqueous HF–HBrO₄ solutions for wet-chemical etching of (100) silicon wafer surfaces

Nils Schubert, ^{ac} Niklas Zomack, ^{ac} André Stapf, ^{ac} Patrick Fuzon, ^b
Ann-Lucia Neumann, ^{ac} Dominic Walter, ^d Andreas Lißner, ^d
Florian Kraus ^b and Edwin Kroke ^{*ac}

Aqueous solutions of hydrofluoric acid (HF) and perbromic acid (HBrO₄) are investigated as nitrogen oxide (NO_x)-free mixtures for wet-chemical etching of (100) silicon wafer surfaces. For the high amount of HBrO₄ needed in this work, an improved synthesis for HBrO₄ with less consumption of fluorine (F₂) is reported. We investigated etching mixtures containing HF in the range of 14–22 mol L⁻¹ and HBrO₄ in the range of 0.25–0.5 mol L⁻¹. These mixtures are polishing silicon surfaces with high etch rates of up to 2 μm min⁻¹ at room temperature. Increasing the temperature leads to higher etch rates up to 7.8 μm min⁻¹. Resulting morphologies on treated silicon surfaces are investigated by scanning electron microscopy (SEM), confocal laser scanning microscopy (CLSM), X-ray photoelectron spectroscopy (XPS) and diffuse reflectance infrared Fourier transform spectroscopy (DRIFTS). The results indicate a reaction pathway with silicon surfaces oxidized by inserting oxygen into Si–Si-bonds by HBrO₄. The reduction of HBrO₄ leads to multiple Br-species in equilibria, thus altering the etching behavior and leading to different surface morphologies.

Received 8th December 2025,
Accepted 16th February 2026

DOI: 10.1039/d5ma01429h

rsc.li/materials-advances

1. Introduction

For the industrial application of silicon substrates, Si surfaces have to be cleaned and etched, *e.g.* for photovoltaics or microelectronics.¹ Wet-chemical processes are used in mass-production of *e.g.* solar cells or microchips, because of their low cost, easiness of use and high throughput. Isotropic etching is used for saw damage removal (SDR) or polishing of monocrystalline silicon surfaces. Mixtures of hydrofluoric acid (HF) and nitric acid (HNO₃) are established in the industry.² The etching mechanism in acidic HF solutions is generally described as a two-step process of silicon oxidation followed by complexation by HF.³ Etching in aqueous HF–HNO₃ solutions generates very smooth surfaces and because of the high reactivity towards silicon, process times are short but the etchant has to be cooled.^{4,5} Additionally, the chemicals are available in high purity, which is beneficial for the electronic properties of the product, *e.g.* solar cells or microchips.⁶ Some contaminants are

able to diffuse from the silicon surface into the bulk (*e.g.* Cu-atoms), thus reducing the minority-carrier lifetime, which is especially undesirable in the photovoltaics industry.¹ Etching silicon in aqueous HF–HNO₃ solutions releases toxic gaseous nitrogen oxides (NO_x) and aqueous waste solutions containing high amounts of nitrate ions (NO₃⁻) in addition to further toxic species which have to be disposed of.⁷ Metal-assisted chemical etching (MACE) can be used to achieve surface structuring with HF solutions.⁸ By using a precious metal (*e.g.*, Cu, Ag) in combination with an oxidizing agent (*e.g.*, H₂O₂) in HF solution, inverted pyramidal structures can be generated on monocrystalline (100) Si wafers.⁹ An alternative route uses alkaline etchants like sodium hydroxide (NaOH), potassium hydroxide (KOH) or tetramethylammonium hydroxide (TMAH).¹⁰ Those etchants are dissolving silicon anisotropically, leading to rougher surfaces compared to acidic processes.^{11,12} Usually, surfactants like isopropyl alcohol (IPA) or Triton X-100 (a non-ionic surfactant) are added to optimize selectivity and homogeneity of the resulting surface texture.^{13,14} The reactivity of alkaline etching mixtures towards silicon is much lower, which requires heating of the solutions to ~80 °C.¹⁵ On the other hand, using NaOH or KOH solutions has a much smaller environmental impact compared to the acidic process, but the chemicals are not available in very high purity.¹ Table 1 shows etch rates of different acidic and alkaline etchants for monocrystalline silicon wafers.

Our working group is aiming to replace HNO₃ as oxidant for the development of acidic etchants for silicon with less

^a Institute of Inorganic Chemistry, Technische Universität Bergakademie Freiberg, Leipziger Str. 29, D-09599 Freiberg, Germany.
E-mail: edwin.kroke@chemie.tu-freiberg.de

^b Research Group for Inorganic Chemistry, Philipps-University of Marburg, Hans-Meerwein-Strasse 4, D-35043 Marburg, Germany

^c Centre for Efficient High-Temperature Material Conversion, Technische Universität Bergakademie Freiberg, Winklerstr. 5, D-09599 Freiberg, Germany

^d Institute of Physical Chemistry, Technische Universität Bergakademie Freiberg, Leipziger Str. 29, D-09599 Freiberg, Germany



Table 1 Etch rates of typical etching solutions on (100) silicon surfaces

Etchant	Temperature	Etch rate [$\mu\text{m min}^{-1}$]	Literature
HF-HNO ₃	20 °C	> 180	4
HF-HNO ₃ -CH ₃ COOH	25 °C	28.0	16
HF-Cl ₂	20 °C	0.8	17
HF-HCl-Cl ₂	20 °C	0.63	18
HF-HClO ₃	20 °C	0.12	19
HF-HClO ₄	20 °C	0.019	20
HF-Br ₂	20 °C	4.0	21
HF-HBr-Br ₂	20 °C	2.0	21
HF-HBrO ₃	20 °C	10.0	22
HF-H ₂ O ₂	20 °C	0.0012	23
HF-O ₃	20 °C	0.05	24
NaOH-IPA	84 °C	0.9	25
KOH-Triton X-100	75 °C	0.65	14
TMAH-Triton X-100	90 °C	0.7	26

The etching rate was within the measurement deviation in this case.

environmental impact. We therefore used aqueous solutions of HF in combination with the halogens chlorine (Cl₂) and bromine (Br₂) as oxidants. Aqueous HF-X₂ (X = Cl, Br) solutions are isotropic etchants, polishing monocrystalline silicon surfaces with high reactivities at room temperature.^{18,21} The addition of the corresponding hydrohalic acid (HCl or HBr) to HF-X₂ mixtures leads to anisotropic etching and therefore texturization of (100) silicon surfaces with canyons, upright or inverted pyramidal structures.^{17,18,21} The process of silicon dissolution in these solutions is not yet fully understood, which is why we are currently investigating the etching behavior of HF solutions with halogen oxoacids as oxidants towards silicon. Generally, silicon oxidation takes place *via* induction of holes (h⁺) into the silicon valence band, which requires oxidants with an electrode potential above +0.7 V.²⁷

Solutions of HF and bromic acid (HBrO₃) are dissolving silicon very fast and polished surfaces are obtained.²² Etching silicon in aqueous HF-HBrO₃ mixtures is accompanied by the formation of Br₂, which is also an active oxidizing agent leading to silicon dissolution. The system shifts into a texturing regime over longer etching periods, leading to matt surfaces. We assume that formed polybromides are the cause for the anisotropic silicon dissolution. With chloric acid (HClO₃), polished surfaces are also obtained, but the reactivity towards silicon is much lower (see Table 1).¹⁹ The polishing regime in the HF-HClO₃ etching system is much more resilient, structured surfaces are only obtained if HCl is added to the solution.¹⁹

The reaction behavior of silicon in aqueous solutions of HF and perchloric acid (HClO₄) has been studied recently.²⁰ No silicon dissolution is observed because the etching reaction is kinetically inhibited. HClO₄ is a strong oxidizer with a redox potential of $E^\circ(\text{ClO}_4^-/\text{Cl}^-) = +1.38 \text{ V}$ (pH = 0),²⁸ but the perchlorate ion (ClO₄⁻) is a very weak nucleophile, which explains the observed reaction behavior.²⁰ The relatively small chlorine atom in the perchlorate anion is very effectively shielded by the four oxygen atoms. Since bromine atoms are significantly larger, the shielding should be less effective, leading to higher reactivity. Periodic acid (H₅IO₆) has not yet been studied for wet-chemical etching of silicon, but for Ruthenium (Ru) etching.²⁹ Since the central iodine atom in HIO₄ is very large, additional oxygen

atoms are attached, which is why HIO₄ does not exist in aqueous solution and is converted to H₅IO₆.²⁸ Studies on the use of H₅IO₆ as oxidizer in the chemical-mechanical polishing (CMP) slurry for silicon carbide (SiC) removal have been carried out.³⁰ The reaction properties of perbromic acid (HBrO₄) are intermediate between these of HClO₄ and H₅IO₆, it is described as a sluggish oxidant at room temperature, but reacts fairly rapidly at 100 °C.³¹ Therefore, it was unclear if silicon dissolution actually occurs in aqueous HF-HBrO₄ solutions.

In this work, we report on aqueous solutions containing HF and HBrO₄ as acidic etchants suitable for fast dissolution of silicon at room temperature. The reactivity was also tested at elevated temperatures of up to 100 °C. Generated reaction products and silicon surface morphologies are discussed as well as silicon dissolution rates. We analyzed the silicon surface after oxidation with HBrO₄ and after etching in HF-HBrO₄ solution *via* diffuse reflectance infrared Fourier transform spectroscopy (DRIFTS) and X-ray photoelectron spectroscopy (XPS). The results are discussed in the context of existing models for silicon dissolution in acidic media.

2. Experimental

2.1. Materials and methods

2.1.1. Chemicals and materials. For the preparation of the etching solutions, HF (50 wt%, VLSI, Honeywell), and deionized (DI) water were used. HBrO₄ is not commercially available.³² It was prepared by passing gaseous fluorine (F₂/N₂ 20:80, v/v, Solvay) into a strongly alkaline (NaOH, >99%, p.a., Carl Roth) solution of sodium bromate (NaBrO₃, >99%, p.a., Carl Roth). The crude product was extracted with acetone (C₃H₆O, technical purity) and evaporated to dryness. The resulting sodium perbromate monohydrate (NaBrO₄·H₂O) was dissolved in DI water and passed over a strong acid cation exchange resin (Amberlite™ HPR1100, Sigma Aldrich) to yield the corresponding acid. The ion exchange resin was loaded with H⁺-ions by conditioning with diluted sulfuric acid (prepared from concentrated H₂SO₄, 96 wt%, VLSI, Honeywell). The prepared HBrO₄ had a concentration of 1 mol L⁻¹. When storing the acid at room temperature for several months, a light-yellow coloration appeared due to decomposition of a very small bromate content (formation of Br₂). This can be removed by bubbling N₂ into the solution for several minutes. For the determination of the etch rates, silicon wafer pieces of approximately 1 cm × 1 cm ((100 orientation), boron doped, as-cut diamond wire sawn, thickness of 180 μm, resistivity of 1.75 Ω cm⁻¹, SolarWorld Industries Thüringen GmbH, Germany) were used. Detailed information on the investigated compositions of the etching solution and the observed etching rates are to be found in the SI (Table S1).

2.1.2. Determination of etching rates. The etch rate r is the quotient of the removed silicon layer thickness per side (Δd) and the immersion time (t_{etch}), see eqn (3). The thickness of the removed silicon layer per side (Δd) is calculated from the mass loss obtained by differential weighing ($\rho_{\text{Si}} = 2.336 \text{ g cm}^{-3}$ at 20 °C),³³ see eqn (2). To determine the area of the wafer fragment,



the total area of the wafer and its mass were determined. From this, the area of the fragment can be calculated using eqn (1).

$$A_0 = \frac{A_{\text{wafer}} \times m_0}{m_{\text{wafer}}} \quad (1)$$

$$\Delta d = d_0 - d_1 = \frac{(m_0 - m_1) \times 10^4}{2 \times \rho_{\text{Si}} \times A_0} \quad (2)$$

$$r = \frac{\Delta d}{t_{\text{etch}}} \text{ in } (\mu\text{m min}^{-1}) \quad (3)$$

A_0 = area of the wafer piece (cm^2), A_{wafer} = area of the wafer (cm^2), m_0 = mass of the wafer piece (g), m_{wafer} = mass of the wafer (g), d_0 = thickness before etching (μm), d_1 = thickness after etching (μm), m_1 = mass of the wafer piece after etching (g), ρ = density (g cm^{-3}), t_{etch} = etching time (min).

2.1.3. Characterization of treated silicon wafers. SEM measurements were carried out with a Tescan Vega TS 5130 S B system. CLSM investigations were carried out with a Keyence VK-X3000 device. For the XPS measurements, a Specs Phoibos 150 CCD-9 spectrometer was used with an Al- K_{α} source (1486.71 eV) in a vacuum of less than 10^{-9} mbar. One scan was recorded for the survey measurement, while the detailed spectra (Si 2p, C 1s, O 1s, F 1s & Br 3d) were averaged from 20 individual scans. The measurements were carried out with the use of a flood gun. Treated wafer pieces for the XPS-measurements were not rinsed with DI water to avoid altering the surface termination and instead dried immediately with N_2 after the oxidation or etching. Short exposure to ambient humidity was inevitable during handling of the wafer fragments in ambient conditions. Due to the direct insertion into the XPS chamber, the sample had minimal contact with air. The energy scales for all spectra were calibrated by setting the signal of adventitious carbon to 284.8 eV.³⁴ A Thermo Fisher Scientific Nicolet iS50 FTIR spectrometer with Smart Collector Avatar accessory was used for DRIFTS measurements of etched silicon wafers. For each DRIFTS-measurement, 64 scans with a resolution of 0.96 cm^{-1} were collected and averaged.

2.1.4. Characterization of the liquid phase. The liquid phases were investigated by Raman spectroscopy. An Ocean Insight QEP05509 Raman spectrometer with a 785 nm laser source (499 mW) was used. The spectra were acquired at an integration time of 10 s and averaged from 3 scans. The focal point of the laser was set to 7 mm in front of the measuring probe window. The measurement was conducted directly through the wall of the perfluoroalkoxy copolymer (PFA) beaker.

2.1.5. Etching procedure. *Caution!* Etching experiments with hydrofluoric acid and perbromic acid must be performed in a HF- and halogen-approved fume hood with HF- and Br_2 -resistant laboratory equipment.

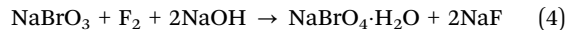
All etching experiments were carried out in PFA beakers. The silicon wafer fragments were held with polytetrafluoroethylene (PTFE) tweezers and placed in the etching solution. During some of the etching experiments, N_2 was bubbled into the etching solution *via* a PTFE frit. The etching reaction was stopped by rinsing the wafer piece with DI water. After rinsing, the wafer pieces were dried with pressurized air.

2.1.6. Oxidation procedure. To H-terminate the silicon surface, as-cut silicon wafer pieces were pretreated by etching in an aqueous mixture containing 11.7 mol L^{-1} HF and 3.9 mol L^{-1} HNO_3 for 5 min. After etching, the wafer pieces were rinsed with DI water and dried with pressurized air. The obtained H-terminated wafer pieces were then placed into the oxidation solution for 1 min, rinsed with DI water and dried with pressurized air.

For the XPS measurements, the wafer pieces were not rinsed with DI water to avoid altering the surface termination, and instead dried immediately with N_2 . Therefore, short exposure to ambient humidity was inevitable during handling of the wafer fragments. In the XPS measurement for the oxidation of an H-terminated silicon surface with aqueous HBrO_4 , the procedure was altered because the acid ran off the wafer very poorly and a lot of perbromate was detected on the wafer during the XPS measurement. Before drying with N_2 , the surface was additionally rinsed with a small amount of acetonitrile. Drying with N_2 afterwards resulted in a dry surface.

2.2. Synthetic procedures

2.2.1. Preparation of $\text{NaBrO}_4 \cdot \text{H}_2\text{O}$. *Caution!* Fluorine must be handled with appropriate protective gear and ready access to proper emergency treatment procedures in case of contact. It can react vigorously to explosively with water.



$\text{NaBrO}_4 \cdot \text{H}_2\text{O}$ was prepared by introducing gaseous fluorine (F_2 , 20 v/v% in N_2) into a strongly alkaline solution of NaBrO_3 . The procedure from G. Brauer³² was modified to reduce the amount of unreacted F_2 leaving the apparatus. A cascade of two scrubber bottles (1000 mL & 500 mL) was used. For the reaction in the first PFA scrubber bottle, 40 g (0.27 mol) of NaBrO_3 were suspended in 400 mL of a 20% NaOH solution. To the second scrubber bottle, a suspension of 20 g (0.13 mol) NaBrO_3 in 200 mL 20% NaOH solution was added. Under ice cooling, 20 v/v% fluorine gas in nitrogen was passed through the bottles into the reaction solutions for a total of 6 h. The reaction is highly exothermic, causing the mixture to boil despite ice cooling. An inlet tube with a diameter of at least 9 mm should be selected here, as the standard 5 mm inlet tube quickly got clogged with sodium fluoride (NaF). Significantly lower heat generation is a good indicator that the NaOH has been completely consumed. As soon as all the sodium hydroxide had been neutralized, an additional 60 mL of 50% NaOH solution and an additional 16 g (0.11 mol) of NaBrO_3 were added to the first scrubber bottle. Subsequently, further fluorine gas was introduced. This process was repeated once more with 80 mL of 50% NaOH solution and 20 g (0.13 mol) of NaBrO_3 . The quantities of chemicals used are shown in Table 2. A grayish-white paste-like solid formed as the reaction proceeded. The end of the reaction was monitored by measuring the pH of the solution in the second bottle until it reached neutrality. Excess water was removed at 20 mbar and 60°C by rotary evaporation. The crude product was washed three times with acetone to extract the $\text{NaBrO}_4 \cdot \text{H}_2\text{O}$.^{35,36} The solvent was then removed at 300 mbar and 60°C in a dynamic vacuum. From this



Table 2 Quantities of chemicals used to prepare sodium perbromate

	Compound	Wash bottle 1	Wash bottle 2
Weigh-in	NaOH	400 mL (20%)	200 mL (20%)
	NaBrO ₃	40 g (265 mmol)	20 g (132.5 mmol)
1st addition	NaOH	60 mL (50%)	—
	NaBrO ₃	16 g (106 mmol)	—
2nd addition	NaOH	80 mL (50%)	30 mL (50%)
	NaBrO ₃	20 g (132.5 mmol)	8 g (53 mmol)
3rd addition	NaOH	—	40 mL (50%)
	NaBrO ₃	—	10 g (66.25 mmol)

concentrated solution crystals of the product did not form spontaneously. For this reason, the remaining solution was further dried at 80 °C until the solvent evaporated and the reaction product crystallized. Powder X-ray diffraction confirmed the phase purity (see SI, Fig. S1 and S2). NaBrO₄·H₂O was obtained as a colorless solid with a yield of 16 g (0.087 mol).

2.2.2. Preparation of HBrO₄



HBrO₄ was prepared from NaBrO₄·H₂O by ion exchange according to the preparation published by G. Brauer.³² 500 mL of a strong-acid ion exchange resin (≥ 2.0 eq L⁻¹ total exchange capacity) were suspended in DI-water and loaded into a 500 mL borosilicate glass column (1 eq L⁻¹, this corresponds to four times the stoichiometrically required amount). The ion exchanger loaded with Na⁺ ions was conditioned with 500 mL of 2 molar H₂SO₄, prepared by adding 55.7 mL 96% H₂SO₄ to 444.3 mL of DI water with cooling, which corresponds to a 100% excess. After passing the acid through the column, a strongly acidic solution was obtained at the end of the column, which indicates a complete conditioning with H⁺-ions. 46.38 g (0.25 mol) NaBrO₄·H₂O were dissolved in 250 mL of DI-water, a Raman spectrum of the aqueous NaBrO₄ solution can be found in the SI (Fig. S3). The resulting solution was passed through the column. Three fractions were collected, fraction 1 had a pH of 7 (water from flushing after conditioning with H₂SO₄), fraction 2 was collected as soon as the pH went below 3 and the beaker was swapped again as soon as the pH went above 3, thus collecting fraction 3. Additional DI water was used to flush all of the acid from the column. Fraction 1 and 3 were discarded, the crude HBrO₄ solution (fraction 2) had a volume of 435 mL, a Raman spectrum of the crude HBrO₄ can be found in the SI (Fig. S4). It was concentrated to a volume of 250 mL by rotary evaporation (40 °C, 60 mbar). The resulting perbromic acid had a slight yellow color due to the decomposition of traces of BrO⁻ and BrO₃⁻, which may still be present as impurities after preparation. The contained Br₂ was removed by bubbling N₂ through the solution for several minutes. A small portion of the acid was then titrated with 0.2 molar NaOH solution and bromothymol blue as an indicator. A total acid content of 0.220 mol was determined. The acid was then concentrated to a volume of 220 mL by rotary evaporation. 220 mL of colorless, 1 M HBrO₄ were obtained. An ion chromatogram can be found in the SI (Fig. S5).

3. Results and discussion

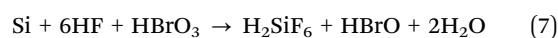
3.1. Reactivity studies

HBrO₄ is a superacid ($\text{p}K_{\text{a}} = -8.5$, $H_0 = -13.8$)³⁷ and a very strong oxidizer, the redox potential $E^\circ(\text{BrO}_4^-/\text{BrO}_3^-) = +1.85$ V²⁸ is high enough to oxidize silicon surface atoms, which requires a potential of at least +0.7 V.³⁸ Nevertheless, a high redox potential does not imply that fast silicon dissolution will actually occur, as kinetic factors play an important role. For example, silicon is not attacked by aqueous HF-HClO₄ solutions, because the perchlorate ion is a very weak nucleophile,²⁰ despite its high redox potential $E^\circ(\text{ClO}_4^-/\text{Cl}^-) = +1.38$ V.²⁸ Because the perbromate ion is a quite inert oxidant with an apparent oxidizing power between perchlorate and periodate, we were unsure about its reactivity towards silicon.³¹

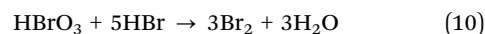
Surprisingly, we observed fast silicon dissolution in aqueous HF-HBrO₄ solutions. First evidence for the etching reaction taking place was the change in color of the etching solution, which was colorless when freshly prepared but quickly changed to orange as silicon was immersed (formation of Br₂). Aqueous HF-Br₂ solutions are known to dissolve silicon with etch rates up to 4 μm min⁻¹,²¹ which is why we aimed to expel formed Br₂ from the etching solution. This was done in order to examine only the reaction behavior of the perbromate as best as possible. We have chosen and combined two methods to remove the volatile bromine: etching at elevated temperatures (b.p. of Br₂ = 58.78 °C)²⁸ and introducing nitrogen (N₂) into the solution. The dissolution of silicon in HF-HBrO₄ solutions is likely taking place according to eqn (6).



As shown in eqn (6), HBrO₃ is formed when HBrO₄ is reduced at the silicon surface. HBrO₃ itself is also capable of dissolving silicon when combined with HF according to eqn (7).²²



The formed hypobromous acid (HBrO) undergoes rapid step-wise decomposition in acidic media according to eqn (8) and (9),³⁹ resulting in the formation of Br₂ because of the synproportionation of bromate and bromide ions according to eqn (10).²⁸ Multiple reactions are taking place at the same time, e.g. bromic acid (HBrO₂) is also decomposing very fast in acidic media.



We determined the etch rates of aqueous HF-HBrO₄ solutions towards (100) silicon wafer surfaces at temperatures between 20 °C to 100 °C, the results are shown in Fig. 1. A total of five silicon wafer pieces were etched one after the other in the same etching solution. The respective wafers (first, second, etc.) were connected with dashed lines for orientation purposes.

The observed etch rate is depending strongly on the etching temperature and seems to reach a maximum around 80 °C. As the concentration of HBrO₄ decreases during etching, the etch



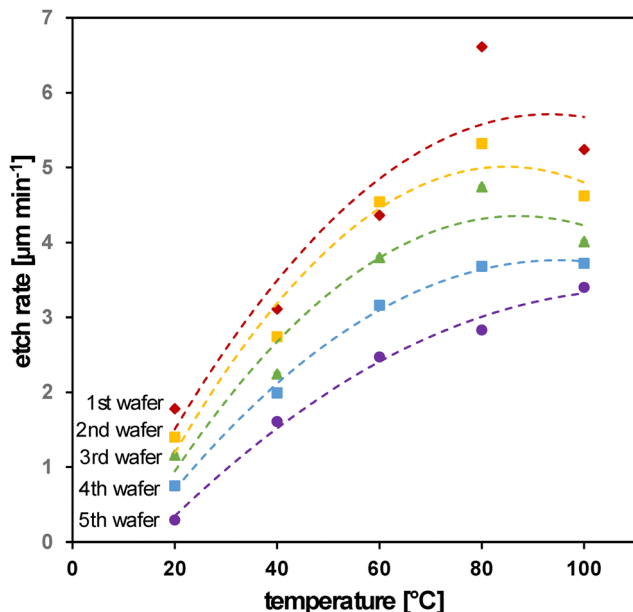


Fig. 1 Etch rates of (100) silicon wafer surfaces vs. etching temperature in aqueous HF–HBrO₄ mixtures between 20 °C to 100 °C with 300 rpm of stirring.

rate also decreases. This can be seen for every tested etching temperature as the later wafer pieces are etched at a reduced rate.

In Fig. 2, the observed etch rate is plotted *versus* the amount of silicon already dissolved in the etching solution. A good fit can be obtained for every tested etching temperature, indicating that the etch rate decreases linearly with the amount of dissolved silicon (and thus the amount of consumed HBrO₄). This suggests that, with the same solution composition, less

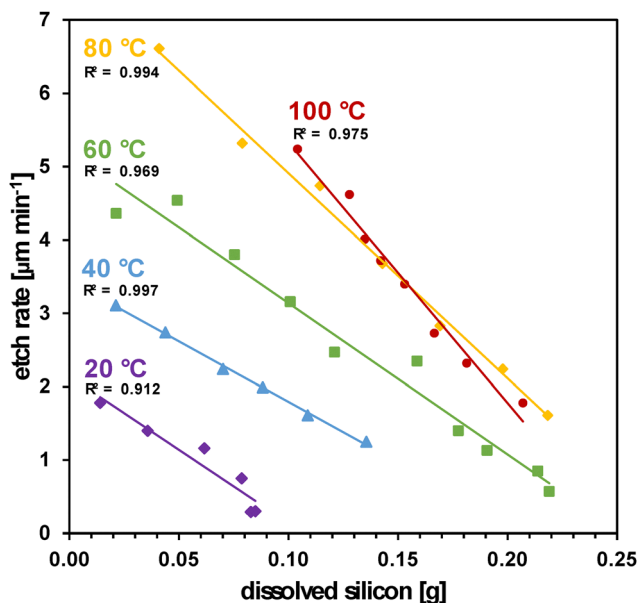


Fig. 2 Etch rates of (100) silicon wafer surfaces vs. the amount of already dissolved silicon in aqueous HF–HBrO₄ mixtures between 20 °C to 100 °C with 300 rpm of stirring.

silicon can be dissolved at 20 °C compared to higher temperatures. We suspect that this is caused by the temperature dependence of the oxidation power of perbromic acid. This implies that no significant silicon dissolution occurs in solutions with low HBrO₄ concentration at room temperature, but there is a reaction when heated. Kinetic factors could be responsible for this effect.

Silicon is dissolved with etch rates up to 2 μm min⁻¹ at room temperature, when the mixture contains 14.6 mol L⁻¹ of HF and 0.5 mol L⁻¹ of HBrO₄. Increasing the temperature of the etching solution accelerates the etching reaction to a maximum of 7.8 μm min⁻¹ at 100 °C (see SI, Table S1, Experiment V.1). The etch rate decreases linearly with the amount of dissolved silicon, because the concentrations of the oxidizing species HBrO₄ and the complexing species HF are decreased. The slope of the functions between 20 to 80 °C is similar, but at 100 °C the etch rate drops faster. We assume additional decomposition reactions of the BrO_x⁻-species taking place at 100 °C leading to a faster decline in the dissolution rate.

Etching of (100) silicon wafer surfaces in freshly prepared aqueous HF–HBrO₄ solutions leads to polished surfaces of high reflectivity. If Br₂ is accumulated in the etching solution, (100) silicon surfaces are partially matt after etching. This change in surface morphology is likely due to anisotropic etching like in aqueous HF–HBr–Br₂ solutions.²¹ The extent of surface texturization is depending on the Br₂ content of the etching solution. Using old HF–HBrO₄ solutions with higher Br₂ contents (which are visibly orange) can lead to surfaces with a very matt appearance. We therefore carried out surface analysis studies using scanning electron microscopy (SEM) to examine the structures generated on (100) silicon surfaces during etching in HF–HBrO₄ solutions.

3.2. Surface morphology

Silicon wafers, etched with aqueous HF–HBrO₄ solutions, were investigated by SEM. Etching at 100 °C expels the formed Br₂ and decomposes the generated HBrO₃. Removing more than the usually about 5 μm deep saw damage¹ results in smooth surfaces. Due to the very small height differences on polished wafers, hardly any surface structures can be seen. Therefore, the SEM images have been moved to the SI (see Fig. S6). We assume aqueous HF–HBrO₄ solutions to be isotropic etchants for (100) Si, making them suitable for saw damage removal (SDR) or polishing of silicon wafers with high reactivities at room temperature and without the generation of gaseous nitrogen oxides (NO_x).

Etching over longer time periods, at lower temperatures or not introducing N₂ into the etching solution leads to the formation of structures on the silicon wafer surface indicating anisotropic etching. In the SEM pictures, very small onsets of texturization become visible, even though the wafer looks very shiny to the naked eye (see SI, Fig. S7). The edge lengths of the generated structures are smaller than 0.50 μm. To improve the visibility of the structures, some of the analyzed surfaces were investigated with confocal laser scanning microscopy (CLSM). As seen in Fig. 3, a lot of very small pyramid tips are formed, thus roughening the surface.

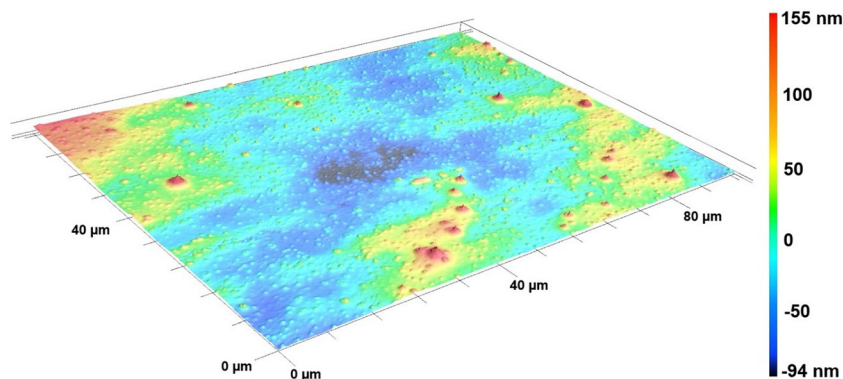


Fig. 3 CLSM image of a silicon (100) surface, etched in a mixture containing $c(\text{HF}) = 14.6 \text{ mol L}^{-1}$, $c(\text{HBrO}_4) = 0.5 \text{ mol L}^{-1}$ at 60°C with N_2 introduction & 300 rpm of stirring for 10 min, $\Delta d = 43.6 \mu\text{m}$.

Reusing old etching solutions also leads to a roughening of the wafer surface as seen in Fig. 4 and 5. Isolated pyramid stumps are generated, which are aligned with the previous saw damage. Etched wafers appear shiny and striped to the naked eye. Etching at room temperature benefits the accumulation of Br_2 in the etching solution, therefore leading to surface texturing with partly fused upright pyramids like in aqueous HF-HBr-Br_2 solutions.²¹ A partly textured surface is shown in Fig. 6, the texturization is also aligned with the previous saw damage.

3.3. DRIFTS measurements of oxidized and etched silicon surfaces

Diffuse reflectance infrared Fourier transform spectroscopy (DRIFTS) experiments were carried out on oxidized and etched surfaces to investigate surface species formed during the oxidation of silicon surfaces with HBrO_4 and etching with HF-HBrO_4 , respectively. Because multiple active species are involved in the etching reaction, different oxidation reactions should occur simultaneously.

$10 \times 10 \text{ mm}$ silicon wafer pieces were H-terminated by etching in a diluted HF-HNO_3 solution (see 2.1.6. Oxidation Procedure). The fragments were then oxidized with HBrO_4 or

etched in HF-HBrO_4 solution, respectively. A DRIFT spectrum of the H-terminated silicon surface is depicted in Fig. 7 (black). Several Si-F absorption bands can be seen around 970 cm^{-1} and 820 cm^{-1} , a partial F-termination after etching in HF containing solutions is well documented in the literature.⁴⁰ The absorption bands around 2100 cm^{-1} and 900 cm^{-1} are characteristic for various Si-H_n groups on the hydrophobized silicon surface.^{41,42} Oxidation of the silicon surface by oxygen-insertion into the Si-Si bonds is known to shift both Si-H bands towards higher wave numbers (e.g. with HNO_3).⁴³ Additionally, H-terminated silicon surfaces show a second band at around 2249 cm^{-1} after oxidation in HNO_3 which is due to still H-terminated surface atoms but with Si-O-Si surface bonds.^{44,45} H-terminated silicon can also be oxidized by the abstraction of hydrogen atoms, which is known from the halogens Cl_2 and Br_2 , thus completely removing the Si-H band.^{21,43,46} DRIFT spectra of H-terminated silicon surfaces, oxidized with HBrO_4 (green) and etched with HF-HBrO_4 (blue) are shown in Fig. 7.

The intensity of the Si-H band at 2117 cm^{-1} is decreasing strongly upon oxidation in aqueous HBrO_4 . The band is slightly shifted to 2125 cm^{-1} and the Si-H deformation band at 903 cm^{-1} is also slightly shifted to 911 cm^{-1} , respectively. Additionally, a very

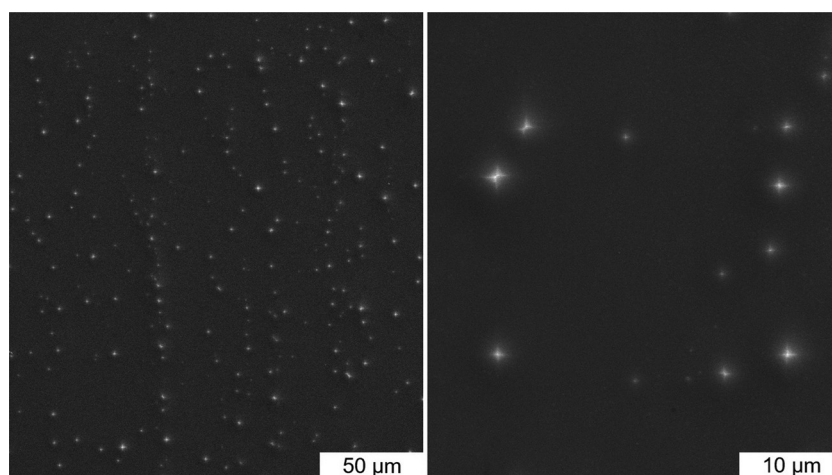


Fig. 4 SEM images of a silicon (100) surface, etched in a mixture containing $c(\text{HF}) = 14.6 \text{ mol L}^{-1}$, $c(\text{HBrO}_4) = 0.5 \text{ mol L}^{-1}$ at 100°C with N_2 introduction, with 300 rpm of stirring for 5 min, $\Delta d = 23.1 \mu\text{m}$.



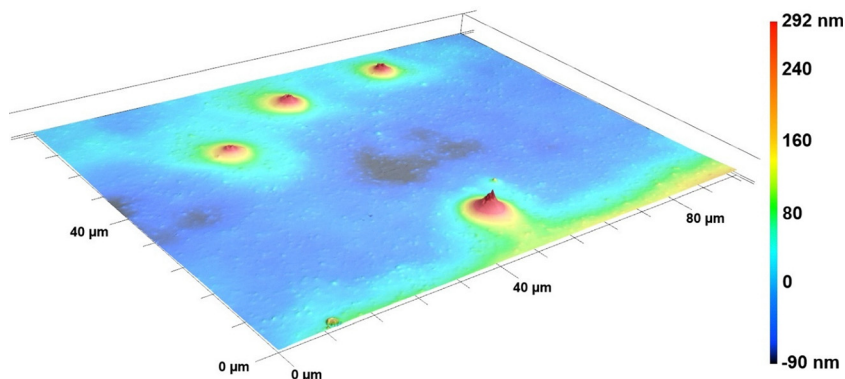


Fig. 5 CLSM image of a silicon (100) surface, etched in a mixture containing $c(\text{HF}) = 14.6 \text{ mol L}^{-1}$, $c(\text{HBrO}_4) = 0.5 \text{ mol L}^{-1}$ at 100°C with N_2 introduction, with 300 rpm of stirring for 5 min, $\Delta d = 23.1 \mu\text{m}$.

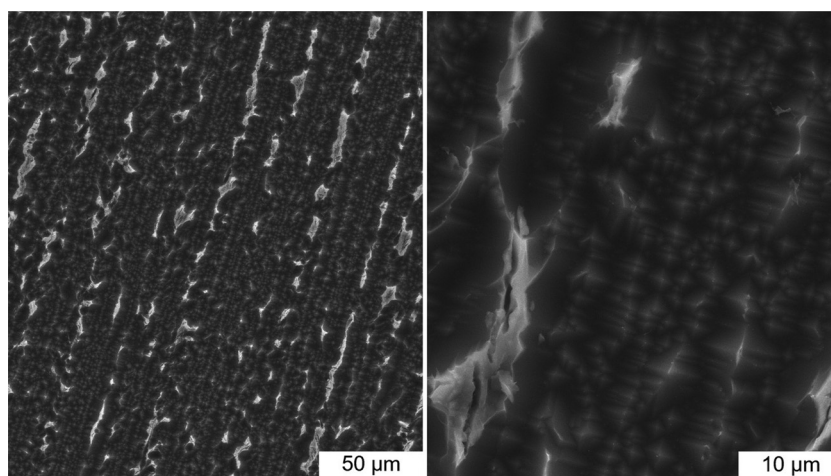


Fig. 6 SEM images of a silicon (100) surface, etched in a mixture containing $c(\text{HF}) = 14.6 \text{ mol L}^{-1}$, $c(\text{HBrO}_4) = 0.5 \text{ mol L}^{-1}$ at 20°C with N_2 introduction, with 300 rpm of stirring for 20 min, $\Delta d = 5.9 \mu\text{m}$.

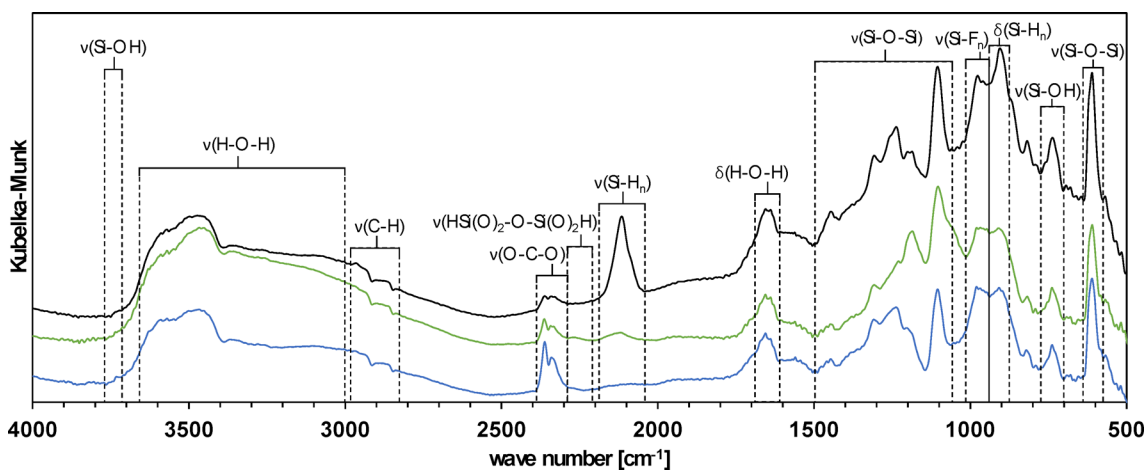


Fig. 7 DRIFT spectra of a silicon (100) surface, H-terminated by etching in HF-HNO_3 for 5 min (black), oxidized with HBrO_4 (green) and etched with HF-HBrO_4 (blue), reaction time was 1 min at room temperature and constant stirring of 300 rpm, see Table S2 in the SI for detailed information about band positions and assignments.



small band appears at 2270 cm^{-1} , indicating $\text{Si(O)}_x\text{-H}$ groups. This behavior is an indication of an oxygen insertion into the Si-Si bonds close to the surface. The strong intensity decrease of the Si-H band around 2100 cm^{-1} is also known from other oxygen-inserting oxidants like HNO_3 or hydrogen peroxide (H_2O_2).²³ A minor Br_2 content due to decomposition reactions could also be responsible for an intensity decrease of the Si-H band around 2100 cm^{-1} .²¹ After etching H-terminated silicon surfaces in aqueous HF-HBrO₄ solutions, the Si-H band is barely visible. This is probably because Br_2 is formed in the reaction, which attacks the Si-H bond very fast.²¹ The structure of the Si-O-Si region between 1050 cm^{-1} to 1500 cm^{-1} is similar to the H-terminated fragment produced by etching in aqueous HF-HNO₃ solution. We therefore assume the surface to initially be H-terminated after etching. This H-termination may also be attacked by the evolving gas phase containing Br_2 , when removing the wafer piece from the etching solution. To generate a

stable H-terminated surface after etching, a subsequent HF dip should follow.

3.4. XPS measurements of oxidized and etched silicon surfaces

H-Terminated silicon wafers were analyzed by X-ray photoelectron spectroscopy (XPS) to investigate different surface species after oxidation with HBrO_4 (see Fig. 8) or etching in HF-HBrO₄ solutions (see Fig. 9). After the oxidation with an aqueous HBrO_4 solution, the sample has a high oxygen content as indicated by the high oxygen-to-silicon-ratio (see Table 5). The oxygen content is significantly lower compared to the oxidation in aqueous HNO_3 .²¹ The Si 2p XPS signal was further analyzed to identify and semi-quantify the surface species bound to silicon. The Si 2p spectrum was processed by using a Shirley-shaped background. The $2p_{1/2}$ spin-orbit component was set to a spin-orbit splitting of 0.61 eV and an intensity ratio ($2p_{1/2} : 2p_{3/2}$) of $1 : 2$.⁴⁷ The Si 2p

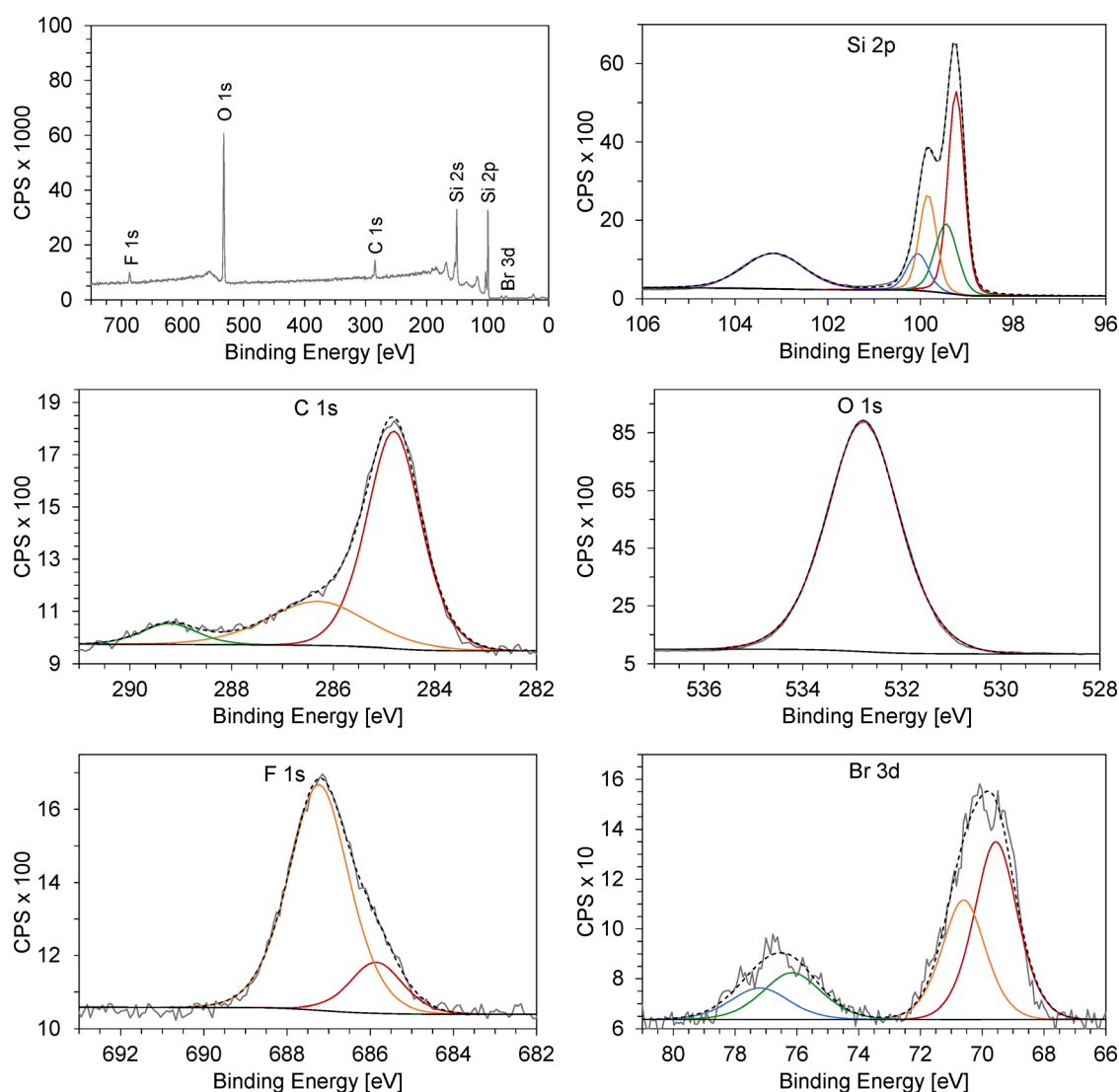


Fig. 8 XPS spectra of a Si(100) surface, preconditioned by etching for 5 min in a HF-HNO₃ mixture containing $c(\text{HF}) = 11.7\text{ mol L}^{-1}$ and $c(\text{HNO}_3) = 3.9\text{ mol L}^{-1}$, followed by oxidation with HBrO_4 , $c(\text{HBrO}_4) = 1.0\text{ mol L}^{-1}$, for 1 min.



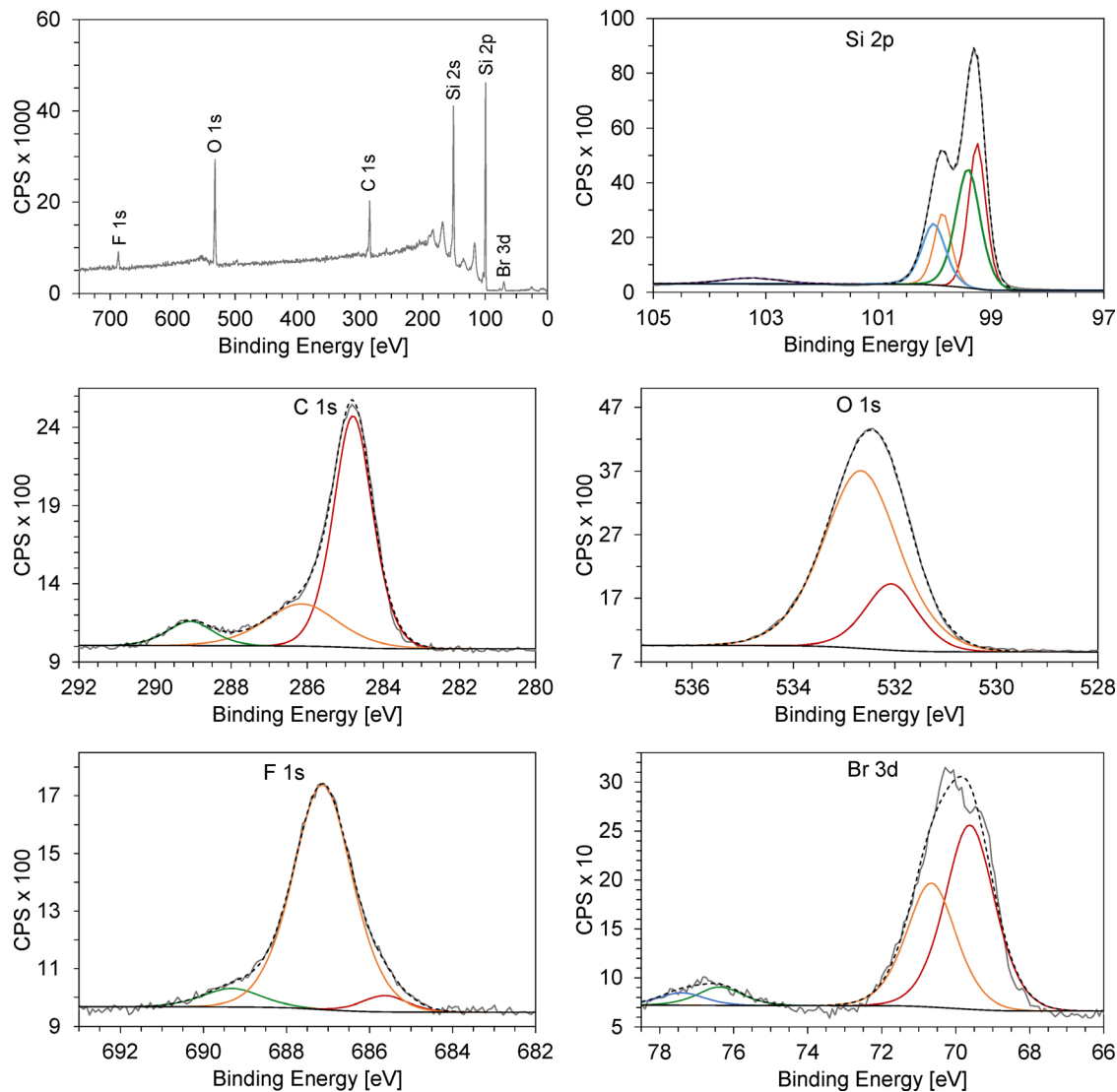


Fig. 9 XPS spectra of a Si(100) surface, preconditioned by etching for 5 min in a HF-HNO₃ mixture containing $c(\text{HF}) = 11.7 \text{ mol L}^{-1}$ and $c(\text{HNO}_3) = 3.9 \text{ mol L}^{-1}$, followed by etching with HF-HBrO₄, $c(\text{HF}) = 14.61 \text{ mol L}^{-1}$, $c(\text{HBrO}_4) = 0.50 \text{ mol L}^{-1}$, for 1 min.

signal was fitted to a total of three species: Si⁽⁰⁾ at 99.24 eV, Si-H at 99.53 eV and Si⁽⁴⁾ at 103.15 eV (see Table 3). The added Si-H species is valued at a binding energy shift (ΔBE) of 0.29 eV, matching with literature data of Si-H₂ groups as also indicated by the DRIFTS measurement (see Fig. 7).⁴⁸ (100) silicon surfaces are characterized by two dangling bonds, which is why Si-H₂ groups are the dominant species on H-terminated (100) wafers.²³ The binding energy shift of the Si⁽⁴⁾ signal is 3.91 eV, which is lower than the observed value for oxidation with HNO₃ (4.21 eV).²¹

The C 1s spectrum was fitted to a total of three species, matching literature data for carbon-containing contaminations, likely due to the handling of the treated fragments in air. In the O 1s spectrum, a good fit can be obtained with only one species, which matches literature data for SiO₂ (see Table 4).^{49,50} Compared to the amount of C-species, there is a high proportion of silicon dioxide (SiO₂) on the surface, therefore the C-O species are not visible in the O 1s spectrum. The

F 1s spectrum was fitted to two species, matching with literature data for fluorine bound to bulk and oxidized silicon atoms, respectively.⁴⁹ It is well documented in the literature, that etching of silicon in HF-solutions leads to a partial F-termination of the silicon surface,⁴⁰ the fluorine content is likely due to the pre-treatment in HF-HNO₃ solution. The Br 3d XPS signal was also processed further by using a Shirley-shaped background. The 3d_{3/2} spin-orbit component was set to a spin-orbit splitting of 1.04 eV and an intensity ratio (3d_{3/2} : 3d_{5/2}) of 0.671 : 1.⁵¹ In the Br 3d spectrum, two separated signals can be seen, the signal at a binding energy of 69.6 eV is attributed to bromine in oxidation state -1, bound to silicon. The second species is likely perbromate or its primary reduction product bromate (BrO₃⁻), as the acid ran off very poorly and residues stayed on the surface, even when additionally rinsed with acetonitrile. Interestingly, the aforementioned species is shifted to significantly higher binding energies (76.16 eV, see Table 4) compared to the values obtained



Table 3 Experimental data of Si 2p_{3/2} binding energy shifts (Δ BE) compared to literature data. The species percentage, based on the signal area, is given in parentheses

Species	Δ BE [eV] (percentage by peak area, %)					
	Cerofolini <i>et al.</i> ⁴⁸	Cerofolini <i>et al.</i> ⁵⁶	Himpfel <i>et al.</i> ⁴⁷	Sundaravel <i>et al.</i> ⁵⁷	HBrO ₄	HF-HBrO ₄
Si ⁽⁰⁾	0.00 (BE _{abs} = 99.30 eV)	0.00 (BE _{abs} = 99.40 eV)	0.00 (BE _{abs} = 99.50 eV)	0.00 (BE _{abs} = 99.30 eV)	0.00 (BE _{abs} = 99.24 eV, 59.65)	0.00 (BE _{abs} = 99.25 eV, 44.57)
Si ^(SiH)	0.13	0.30				0.16 (51.66)
Si ^(SiH₂)	0.28	0.57			0.29 (17.77)	
Si ^(SiH₃)	0.47					
Si ⁽¹⁾	1.01		0.95	1.00		
Si ⁽²⁾	1.84		1.75	2.00		
Si ⁽³⁾	2.86		2.48	2.90		
Si ⁽⁴⁾	3.63		3.90	3.70	3.91 (22.57)	4.00 (3.77)

Table 4 Experimental data of Br-, F-, O- & C-XPS-signals compared to literature data

Species	BE [eV]							
	Jin <i>et al.</i> ⁵⁸	Newberg <i>et al.</i> ⁵²	Sekar <i>et al.</i> ⁴⁹	Lu <i>et al.</i> ⁵⁹	Yue <i>et al.</i> ⁶⁰	Thøgersen <i>et al.</i> ⁵⁰	HBrO ₄	HF-HBrO ₄
3d _{5/2} Br ^(Si-Br)	69.1						69.56	69.62
3d _{5/2} Br ^(C-Br)	70.1							
3d _{5/2} Br ^(O₂-Br)		72.3						
3d _{5/2} Br ^(O₃-Br)		74.6					76.16	76.37
1s F ^(Si-F weak)			684.9					
1s F ^(Si-O-Si-F)			686.4				685.86	685.63
1s F ^(Si-F)			687.5				687.23	687.13
1s F ^(C-F)				689.6				689.32
1s O ^(C=O)					531.2–531.6			
1s O ^(C-O)					532.2–533.4			532.07
1s O ^(O₂ or H₂O)					534.6–535.4			
1s O ^(SiO₂)			531.5			533.05	532.78	532.67
1s C ^(C)					284.6		284.80	284.80
1s C ^(C-H)	284.5		284.0	285.0				
1s C ^(C-O)	286.0		286.2		286.1–286.3		286.31	286.15
1s C ^(C=O keto)	288.8		288.4		287.3–287.6			
1s C ^(C=O acid)					288.4–288.9		289.22	289.08
1s C ^(CO or CO₂)					290.4–290.8			
1s C ^(C-F)				292.4				

by Wagner and Newberg for bromate (74.6 eV).^{52,53} Feng *et al.* reported a binding energy of 76.7 eV for the entire (unsplit) bromate signal which matches our results (76.50 eV) very well.⁵⁴ Hutson *et al.* attribute signals between 76–78 eV to bromate and perbromate species.⁵⁵ Therefore, it cannot be said with certainty which Br-O species is present on the surface. Our experiments with HF-HBrO₃ solutions showed no Br-O species bound to silicon in the XPS measurements after oxidation or etching.²² We therefore assume the detected species to be perbromate.

After etching a H-terminated wafer piece in aqueous HF-HBrO₄ solution, the obtained XPS spectra change and a significantly lower oxygen-content is observed because of the etching by HF. A small signal for Si⁽⁴⁾ is still observed in the Si 2p spectrum at a Δ BE of 4.00 eV (see Table 3), which is not expected when the piece is treated in HF solutions. During the etching reaction, Br₂ is formed and evolving from the solution. We believe that gaseous bromine is oxidizing the wafer piece after its removal from the etching solution, where no HF is present to dissolve oxidized silicon atoms, thus causing the oxidation signal. We also fitted a Si-H species at a Δ BE of 0.16 eV to obtain a good overall fit. The Si-H species has a significantly higher area proportion compared to the Si-H₂ species on the wafer piece only oxidized by HBrO₄ (see Table 3)

and matches well with literature data for monohydride Si-H species.⁴⁸ When (100) Si surfaces are etched with anisotropic etchants, the (100) and (110) planes are dissolved fast and (111) planes remain.¹ Because the formed Br₂ was not removed, the wafer piece had a matt appearance due to the onset of texturization like in aqueous HF-HBr-Br₂ solutions.²¹ The remaining (111) planes are characterized by three silicon-silicon bonds and only one dangling bond, resulting in the observed monohydride species. We therefore believe that the silicon surface is H-terminated after etching, but is attacked very fast by the formed bromine, thus resulting in more hydrophilic surface species like Si-OH. The C 1s and O 1s spectra are fitted to three and two species, respectively and can be assigned to carbon containing contaminations from the handling in ambient conditions and SiO₂ from oxidation or reaction with ambient humidity. At 689.32 eV the F 1s spectrum, a small species can be fitted with good agreement to literature data of C-F bonding, which might be due to contaminations from handling the wafer fragments with PTFE tweezers. Additionally, two species for Si-F bonding are observed, a small one for fluorine bound to oxidized silicon atoms and a large signal for fluorine bound to silicon. In the Br 3d spectrum, a small signal for perbromate is observed at 76.75 eV together with the bromide-signal at 69.62 eV (Br 3d_{5/2}). The wafer piece was not additionally



atom, it should be much easier to attack. In addition, the perbromate ion is more easily polarizable due to its larger central atom.

Oxidation experiments show that HBrO_4 is an oxygen-inserting oxidant, therefore not directly attacking Si–H surface groups, but oxidizing the surface by the formation of Si–O–Si species. This correlates with the polishing nature of the etchant and is very similar for *e.g.* HNO_3 or HBrO_3 , which are also oxygen-inserting and polishing (100) Si surfaces when combined with HF. The perbromate ion is strongly adsorbed to the oxidized or etched silicon surfaces, as a quick rinse with water or acetonitrile does not fully remove the adsorbed species.

Future studies should focus on carrying out *in situ* DRIFTS measurements to possibly detect an intermediate species during etching. The exact Br_2 concentration causing the etching behavior to change from isotropic to anisotropic should also be investigated in detail.

Author contributions

N. S.: data curation, formal analysis, investigation, methodology, validation, visualization, writing–original draft. N. Z.: data curation, formal analysis, investigation, methodology, supervision, validation, writing – review & editing. A. S.: conceptualization, funding acquisition, methodology, project administration, resources, supervision, writing – review & editing. P. F.: supervision, investigation, methodology, validation, writing – original draft. A.-L. N.: data curation, formal analysis, investigation, methodology, validation, visualization, writing – review & editing. D. W.: data curation, formal analysis, investigation, software, writing – review & editing. A. L.: data curation, formal analysis, investigation, software, writing – review & editing. F. K.: resources, supervision, writing – review & editing. E. K.: conceptualization, funding acquisition, project administration, resources, supervision, writing – review & editing.

Conflicts of interest

There are no conflicts to declare.

Data availability

The data supporting this article have been included as part of the supplementary information (SI). The SI contains data of the prepared HBrO_4 , additional SEM images, data of the etching experiments in aqueous HF- HBrO_4 solutions and additional information regarding DRIFTS measurements. Ref. 64 and 65 are cited in the SI. Supplementary information is available. See DOI: <https://doi.org/10.1039/d5ma01429h>.

Acknowledgements

The authors thank the German Research Foundation (DFG) for funding within the project 461795804 (KR1739/38-1). We thank Solvay for the donation of diluted fluorine gas.

References

- 1 A. Stapf, C. Gondek, E. Kroke and G. Roewer in *Handbook of Photovoltaic Silicon*, ed. D. Yang, Springer Berlin Heidelberg, Berlin, Heidelberg, 2018, pp. 1–48.
- 2 J. Acker, T. Koschwitz, B. Meinel, R. Heinemann and C. Blocks, *Energy Proc.*, 2013, **38**, 223.
- 3 H. Robbins and B. Schwartz, *J. Electrochem. Soc.*, 1959, **106**, 505.
- 4 I. Röver, G. Roewer, K. Bohmhammel and K. Wambach, *Freiberg. Forschungsh.*, 2004, 179.
- 5 W. Li, B. Liu, F. Jiao and W. Liu, *Sep. Purif. Technol.*, 2025, **361**, 131414.
- 6 I. Fernández-Olmo, J. L. Fernández and A. Irabien, *Sep. Purif. Technol.*, 2007, **56**, 118.
- 7 M. Lippold, S. Patzig-Klein and E. Kroke, *Z. Naturforsch., B: J. Chem. Sci.*, 2011, **66**, 155.
- 8 F. Honeit, C. Thiele, C. Gondek, N. Schubert, A. Stapf and E. Kroke, *Eur. J. Inorg. Chem.*, 2026, e202500547.
- 9 D. Zhang, L. Wang, R. Jia, K. Tao, S. Jiang, H. Ge, B. Wang, Z. Gao, X. Li and M. Li, *Mater. Sci. Semicond. Process.*, 2022, **138**, 106281.
- 10 P. Pal, V. Swarnalatha, A. V. N. Rao, A. K. Pandey, H. Tanaka and K. Sato, *Micro Nano Syst. Lett.*, 2021, **9**, 4.
- 11 U. Hilleringmann, *Silicon Semiconductor Technology*, Springer Fachmedien Wiesbaden, Wiesbaden, 2023.
- 12 Y. Wang, F. Xi, K. Wei, Z. Tong, S. Li, Z. Ding and W. Ma, *Appl. Energy*, 2025, **386**, 125591.
- 13 N. Burham, A. A. Hamzah and B. Y. Majlis, *2015 IEEE Regional Symposium on Micro and Nanoelectronics (RSM)*, IEEE, 2015, pp. 1–4.
- 14 K. P. Rola and I. Zubel, *J. Microelectromech. Syst.*, 2013, **22**, 1373.
- 15 H. Seidel, L. Csepregi, A. Heuberger and H. Baumgärtel, *J. Electrochem. Soc.*, 1990, **137**, 3612.
- 16 C. Kok Sheng, R. Aarif, A. Ghapur, E. Ali, E. Abd Ghapur and M. Hassan, *J. Sustainability Sci. Manage.*, 2020, **15**, 6.
- 17 A. Stapf, N. Zomack, C. Bellmann, N. Schubert, A.-L. Neumann, F. Buchholz, T. Kollek, A. Helfricht, M. Mohammadi and A. Weber, *et al.*, *IEEE J. Photovoltaics*, 2024, **14**, 414.
- 18 A. Stapf, P. Nattrodt, C. Gondek and E. Kroke, *Phys. Status Solidi A*, 2017, 214.
- 19 A.-L. Neumann, N. Schubert, A. Stapf, N. Zomack and E. Kroke, *Wet chemical etching of silicon wafers with aqueous HF-(HCl)- HClO_3 mixtures. Poster, 41st EU PVSEC, 2024*.
- 20 A.-L. Neumann, A. Stapf, N. Schubert, N. Zomack and E. Kroke, *RSC Adv.*, 2025, **15**, 15796.
- 21 N. Schubert, A. Stapf, A. Lißner, N. Zomack, A.-L. Neumann and E. Kroke, *Chem. Inorg. Mater.*, 2024, **3**, 100063.
- 22 N. Schubert, N. Zomack, A.-L. Neumann, A. Stapf, D. Walter, A. Lißner, A. S. Braeuer and E. Kroke, *Adv. Mater. Interfaces*, 2025, **13**(2), e00773.
- 23 C. Gondek, M. Lippold, I. Röver, K. Bohmhammel and E. Kroke, *J. Phys. Chem. C*, 2014, **118**, 2044.
- 24 C. Gondek, R. Hanich, F. Honeit, A. Lißner, A. Stapf and E. Kroke, *J. Phys. Chem. C*, 2016, **120**, 22349.



- 25 E. Vazsonyi, K. de Clercq, R. Einhaus, E. van Kerschaver, K. Said, J. Poortmans, J. Szlufcik and J. Nijs, *Sol. Energy Mater. Sol. Cells*, 1999, **57**, 179.
- 26 D. Resnik, D. Vrtacnik, U. Aljancic, M. Mozek and S. Amon, *J. Micromech. Microeng.*, 2005, **15**, 1174.
- 27 K. W. Kolasinski and J. W. Gogola, *Nanoscale Res. Lett.*, 2012, **7**, 323.
- 28 A. F. Holleman, N. Wiberg and E. Wiberg, *Lehrbuch der Anorganischen Chemie*, Walter de Gruyter, 2007.
- 29 Y. Kikkawa, Y. Suzuki, K. Saito, H. Yarimizu, S. Kanamori, T. Sato and T. Nagashima, *Solid State Phenom.*, 2023, **346**, 325.
- 30 H. Nitta, A. Isobe, P. Hong and T. Hirao, *Jpn. J. Appl. Phys.*, 2011, **50**, 46501.
- 31 E. H. Appelman, *Inorg. Chem.*, 1969, **8**, 223.
- 32 G. Brauer, *Handbuch der präparativen anorganischen Chemie*, Enke, Stuttgart, 1975.
- 33 H. Park, S. Kwon, J. S. Lee, H. J. Lim, S. Yoon and D. Kim, *Sol. Energy Mater. Sol. Cells*, 2009, **93**, 1773.
- 34 D. Fang, F. He, J. Xie and L. Xue, *J. Wuhan Univ. Technol., Mater. Sci. Ed.*, 2020, **35**, 711.
- 35 V. V. Gavrilov, V. K. Isupov and I. S. Kirin, *USSR Pat.*, 497220, 1975.
- 36 V. V. Gavrilov and V. K. Isupov, *Russ. Chem. Rev.*, 1980, **49**, 1049.
- 37 L. Stein and E. H. Appelman, *Inorg. Chem.*, 1983, **22**, 3017.
- 38 K. W. Kolasinski, *J. Phys. Chem. C*, 2010, **114**, 22098.
- 39 P. Engel, A. Oplatka and B. Perlmutter-Hayman, *J. Am. Chem. Soc.*, 1954, **76**, 2010.
- 40 M. Lippold, U. Böhme, C. Gondek, M. Kronstein, S. Patzig-Klein, M. Weser and E. Kroke, *Eur. J. Inorg. Chem.*, 2012, 5714.
- 41 Z.-H. Wang, T. Urisu, H. Watanabe, K. Ooi, G. Ranga Rao, S. Nanbu, J. Maki and M. Aoyagi, *Surf. Sci.*, 2005, **575**, 330.
- 42 G. Ranga Rao, Z.-H. Wang, H. Watanabe, M. Aoyagi and T. Urisu, *Surf. Sci.*, 2004, **570**, 178.
- 43 A. Stapf, C. Gondek, M. Lippold and E. Kroke, *ACS Appl. Mater. Interfaces*, 2015, **7**, 8733.
- 44 M. Lippold, *Dissertation*, TU Bergakademie Freiberg, Freiberg, 2014.
- 45 J. R. Weidlein, U. Müller and K. Dehnicke, *Schwingungsfrequenzen. Band 1: Hauptgruppenelmente*, Thieme, Stuttgart, 1981.
- 46 A. Stapf, P. Nattrodt and E. Kroke, *J. Electrochem. Soc.*, 2018, **165**, H3045–H3050.
- 47 F. J. Himpsel, F. R. McFeely, A. Taleb-Ibrahimi, J. A. Yarmoff and G. Hollinger, *Phys. Rev. B: Condens. Matter Mater. Phys.*, 1988, **38**, 6084.
- 48 G. F. Cerofolini, A. Giussani, A. Modelli, D. Mascolo, D. Ruggiero, D. Narducci and E. Romano, *Appl. Surf. Sci.*, 2008, **254**, 5781.
- 49 K. Sekar, G. Kuri, D. P. Mahapatra, B. N. Dev, J. V. Ramana, S. Kumar and V. S. Raju, *Surf. Sci.*, 1994, **302**, 25.
- 50 A. Thøgersen, J. H. Selj and E. S. Marstein, *J. Electrochem. Soc.*, 2012, **159**, D276–D281.
- 51 E. M. Freiburger, J. Steffen, N. J. Waleska-Wellnhofer, A. Harrer, F. Hemauer, V. Schwaab, A. Görling, H.-P. Steinrück and C. Papp, *ChemPhysChem*, 2023, **24**, e202300510.
- 52 J. T. Newberg, T. M. McIntire and J. C. Hemminger, *J. Phys. Chem. A*, 2010, **114**, 9480.
- 53 C. D. Wagner, *J. Vac. Sci. Technol.*, 1978, **15**, 518.
- 54 Z. Feng, N. Chen, C. Feng, C. Fan, H. Wang, Y. Deng and Y. Gao, *Appl. Surf. Sci.*, 2019, **488**, 681.
- 55 N. D. Hutson, B. C. Attwood and K. G. Scheckel, *Environ. Sci. Technol.*, 2007, **41**, 1747.
- 56 G. F. Cerofolini, C. Galati and L. Renna, *Surf. Interface Anal.*, 2003, **35**, 968.
- 57 B. Sundaravel, K. Sekar, G. Kuri, P. V. Satyam, B. N. Dev, S. Bera, S. V. Narasimhan, P. Chakraborty and F. Caccavale, *Appl. Surf. Sci.*, 1999, **137**, 103.
- 58 H. Jin, C. R. Kinser, P. A. Bertin, D. E. Kramer, J. A. Libera, M. C. Hersam, S. T. Nguyen and M. J. Bedzyk, *Langmuir*, 2004, **20**, 6252.
- 59 X. Lu, K. C. Wong, P. C. Wong, K. Mitchell, J. Cotter and D. T. Eadie, *Wear*, 2006, **261**, 1155.
- 60 Z. R. Yue, W. Jiang, L. Wang, S. D. Gardner and C. U. Pittman, *Carbon*, 1999, **37**, 1785.
- 61 U. K. Klänning, J. R. Byberg and K. Sehested, *J. Phys. Chem. A*, 1999, **103**, 5055.
- 62 B. Jaselskis and J. L. Huston, *Anal. Chem.*, 1971, **43**, 581.
- 63 C. Sáez, P. Cañizares, A. Sánchez-Carretero and M. A. Rodrigo, *J. Appl. Electrochem.*, 2010, **40**, 1715.
- 64 H. Schulze, N. Weinstock, A. Müller and G. Vandrish, *Spectrochim. Acta, Part A*, 1973, **29**, 1705.
- 65 J. Rouviere, V. Tabacik and G. Fleury, *Spectrochim. Acta, Part A*, 1973, **29**(2), 229–242.

